

УДК 541.64:537.6

## MAGNETIC POLYSTYRENE NANOCAPSULES WITH CORE–SHELL MORPHOLOGY OBTAINED BY EMULSIFIER-FREE MINIEMULSION POLYMERIZATION<sup>1</sup>

© 2011 г. Mohammad Madani<sup>a</sup>, Naser Sharifi-Sanjani<sup>a</sup>, and Reza Faridi-Majidi<sup>b</sup>

<sup>a</sup>School of Chemistry, University College of Science, University of Tehran,  
Tehran, Iran

<sup>b</sup>Department of Medical Nanotechnology, School of Advanced  
Medical Technologies, Tehran University of Medical Sciences,  
Tehran, Iran

e-mail: mmadani@khayam.ut.ac.ir

Received December 23, 2009

Revised Manuscript Received April 18, 2010

**Abstract**—Nanocapsules containing hexadecane and  $\text{Fe}_3\text{O}_4$  magnetic nanoparticles as core materials and polystyrene as shell were produced in a new method through emulsifier-free miniemulsion polymerization using 2,2'-azobis(2-amidinopropane) dihydrochloride (V-50) as a water-soluble initiator. The effect of some parameters such as the amounts of  $\text{Fe}_3\text{O}_4$  and initiator on morphology of resulting nanocapsules was studied. Transmission electron microscopy showed that the products had latex particles having a size range of about 300–1300 nanometer and both magnetic nanocapsules with core–shell morphology and solid particles. The phase transition temperature and phase transition heat of the produced capsules were determined by differential scanning calorimetric analyses. Thermal properties of the latex were compared with those of magnetic-particles-free latex and with those of latex free of both magnetic particles and hexadecane. Thermogravimetric analysis was also used to confirm the encapsulation and to determine the amounts of hexadecane and  $\text{Fe}_3\text{O}_4$  within the capsules.

### INTRODUCTION

In the last decades, polymeric nanocapsules (core–shell particles) with encapsulated liquid or solid materials have caused increasing attention due to the widespread applications of such nanocapsules as controlled and persistent drug delivery systems in pharmaceutical products [1, 2], protecting light-sensitive material devices [3], functional textiles, liquid crystals, adhesives, insecticides, cosmetics, food, catalysis, spice and dye dispersion industries [4–10].

Among several techniques for the preparation of core–shell particles like two-stage seeded emulsion polymerization [11], interfacial polymerization [12] and solvent evaporation [13], the miniemulsion process has proven to be highly efficient for the encapsulation of solid and liquid materials [14].

Miniemulsion polymerization is therefore particularly attractive for the encapsulation reaction of any compound that can be satisfactorily suspended into the monomer phase [15, 16]. In the present work, we report our preliminary investigations of the preparation of nanocapsules with core ( $\text{Fe}_3\text{O}_4$  magnetic nanoparticles and hexadecane)-shell (polystyrene) morphology. Magnetic polymeric particles have been suggested for a variety of applications, especially in

biological field, such as cell separation [17], site-specific drug delivery [18, 19], and tissue engineering [20] and nucleic acids concentration [21].

Among the magnetic materials with suitable properties, magnetite is the only one that has so far been allowed for use in humans. It is the only magnetic material which is known to be biocompatible, without relevant toxicity in the applied dosing range [22]. It has been shown that magnetite nanoparticles produce enough heat in an alternating magnetic field to be applied in hyperthermia treatment [23].

To improve the properties of the magnetite nanoparticles with regard to iron leakage and aggregation or coagulation, the magnetic nanoparticles can be efficiently encapsulated in a hydrophobic polymer shell [24, 25]. This encapsulation ensures that the shell is not washed off in hydrophilic media, which would result in sedimentation and aggregation of the magnetic core particles. At the same time, high magnetite contents and uniform distribution of magnetite in the polymer can be achieved [25]. The polymer chosen for encapsulation in the studies discussed here is polystyrene, because it is cheap, well-known and can easily be functionalized by copolymerization [26].

Nanocapsule size is usually smaller than  $10^3$  nanometer [27]. The approach to the synthesis of nanocapsules described below is based on the principle of

<sup>1</sup> Статья печатается в представленном авторами виде.

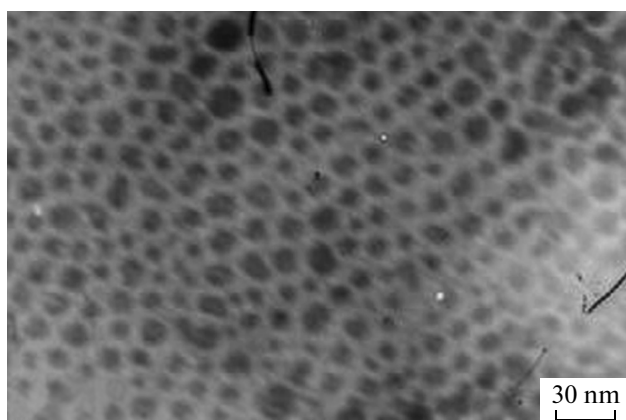


**Fig. 1.** TEM micrographs of the used  $\text{Fe}_3\text{O}_4$  nanoparticles.

emulsifier-free miniemulsion polymerization. Up to now, this kind of process has not been used for the preparation of magnetic nanocapsules.

In this work, encapsulation of magnetite nanoparticles and hexadecane with polystyrene was carried out using a new method based on emulsifier-free miniemulsion polymerization in the presence of 2,2'-azobis(2-amidinopropane) dihydrochloride (V-50) as a cationic ionizable water-soluble initiator and magnetic polymeric nanocapsules were synthesized and characterized by TEM, DSC and TGA.

## EXPERIMENTAL PART

### Materials

The styrene and hexadecane were purchased from Merck Chemical Co. The styrene was purified by distillation under vacuum. The initiator, 2,2'-azobis(2-amidinopropane) dihydrochloride as V-50 was supplied by Organic Acros Co., stored at 4°C and used without further purification. The water was twice distilled. Oleic acid-coated magnetite nanoparticles with an average diameter of about 10 nm (Fig. 1) and containing 21.79 wt % of oleic acid were produced in our

lab according to Reference [28], via coprecipitation of  $\text{Fe}^{+3}$  and  $\text{Fe}^{+2}$  ions in the presence of ammonium hydroxide and oleic acid.

### Miniemulsion Polymerization

The procedure for preparation of magnetic nanocapsules with core ( $\text{Fe}_3\text{O}_4$  magnetic nanoparticles and hexadecane) – shell (polystyrene) morphology via emulsifier-free miniemulsion polymerization was as follows.

Various amounts of hydrophobic  $\text{Fe}_3\text{O}_4$  magnetic nanoparticles, were dispersed in 6.00 g of styrene monomer and these mixtures were sonicated for 50 s to obtain a homogenous dispersion. The resultant stable oil-based dispersion was added to 100 mL of double distilled water containing various amounts of 2,2'-azobis(2-amidinopropane) dihydrochloride (V-50) as an initiator and 6 g of hexadecane. Then the mixtures were sonicated again at 90% output (400 W) for 15 min under argon. During sonication, the temperature of the mixture increased up to around 70–80°C and to prevent the evaporation of the mixture contents, the container was equipped with a condenser. After that, the miniemulsion obtained was polymerized in water bath at 70°C for 6 h. The used recipes for the emulsifier-free miniemulsion polymerizations are given in Table 1 (experiments M1–M4 and R1–R2).

Experiments V and K corresponded to emulsifier-free miniemulsion polymerization of styrene containing no magnetite and emulsifier-free miniemulsion polymerization of styrene free from magnetite and hexadecane, were carried out to compare them with M-series experiments. A CEM 902A ZEISS transmission electron microscope was used. Samples were prepared by placing a droplet (1  $\mu\text{L}$ ) of polymer dispersion, along with a droplet of water, on a copper grid covered by formvar foil (200 mesh), dried and analyzed. Thermal properties of the dried samples were analyzed by TGA (TGAQ50, TA Instruments) and DSC (DSCQ100, TA Instruments) at 20°C/min and 10°C/min for heating rate, respectively, under inert gas of Ar.

## RESULTS AND DISCUSSION

Magnetic nanocapsules with core ( $\text{Fe}_3\text{O}_4$  magnetic nanoparticles and hexadecane)–shell (polystyrene) morphology were prepared via emulsifier-free miniemulsion polymerization method using a cationic water soluble initiator (V-50).

Based on the theories and experimental data, a successful polymer encapsulation of iron oxide particles via miniemulsion polymerization requires these particles to be well dispersed in the monomer before emulsification to be accommodated within the droplets. Since  $\text{Fe}_3\text{O}_4$  nanoparticles are hydrophilic and styrene is a hydrophobic monomer, the polarity difference be-

**Table 1.** Recipes used in emulsifier-free miniemulsion polymerization

Experiment	St., g	Hexade-cane, g	Initiator, g	Added magnetite, g
M1	6	6	0.2	0.05
M2	6	6	0.2	0.2
M3	6	6	0.2	0.3
M4	6	6	0.2	0.5
R1	6	6	0.1	0.3
R2	6	6	0.15	0.3
V	6	6	0.2	0
K	6	0	0.2	0

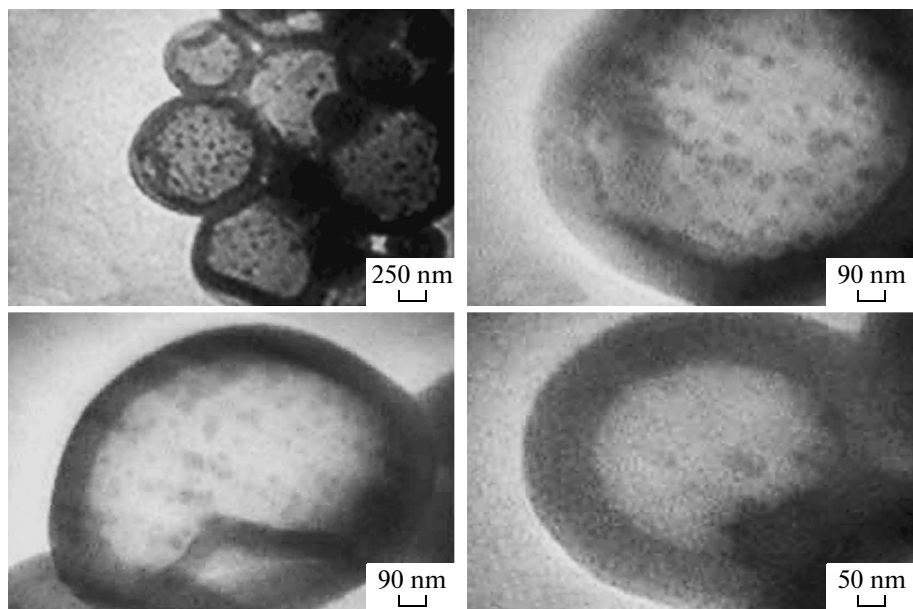


**Fig. 2.** TEM micrographs of the latexes produced in Exp. M4: polystyrene capsules with magnetite and hexadecane core.

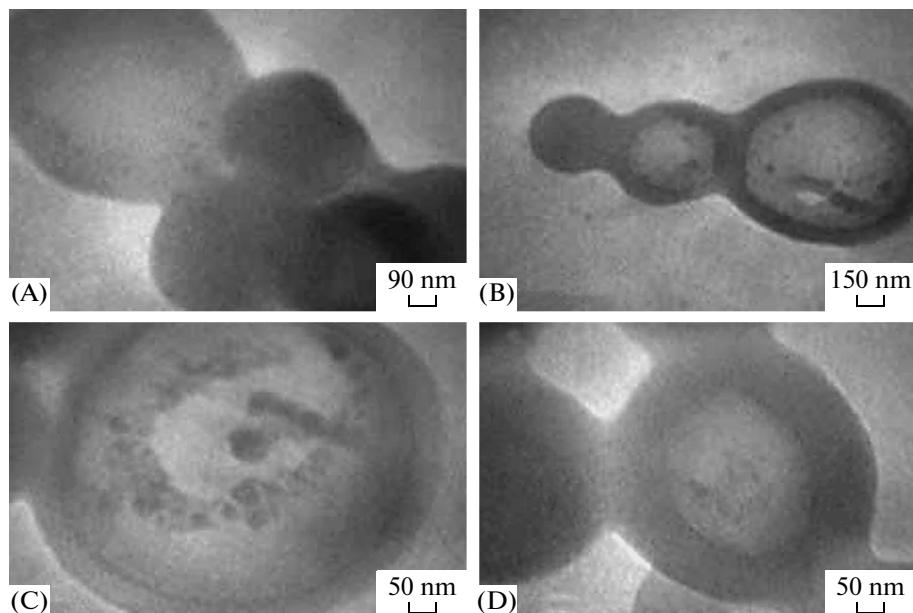


**Fig. 3.** TEM micrographs of the latexes produced in Exp. M3 (A, B) and M2 (C, D).

tween them makes it difficult to disperse iron oxide nanoparticles in styrene without aggregation and phase separation. To improve dispersion, a surface treatment with oleic acid was performed to increase the hydrophobicity of the  $\text{Fe}_3\text{O}_4$  nanoparticles. The average particle size of magnetite prepared in the present study was about 10 nm, which has been estimated by TEM (Fig. 1).

The processes of preparing the magnetic nanocapsules proceed via three stages as described in Experimental Part. To examine the effect of various amounts

of magnetite and initiator on the morphology of the magnetic nanocapsules, a series of miniemulsions were prepared. The hexadecane level was kept constant while the amounts of magnetite and initiator were changed (0.05, 0.2, 0.3, 0.4, and 0.5 g for magnetite and 0.1, 0.15, and 0.2 g for initiator). Subsequent polymerization of the prepared miniemulsion led to production of opaque light brown latex and showed significant encapsulation of hexadecane and  $\text{Fe}_3\text{O}_4$  within the capsules. TEM micrographs of the latex particles obtained from these experiments

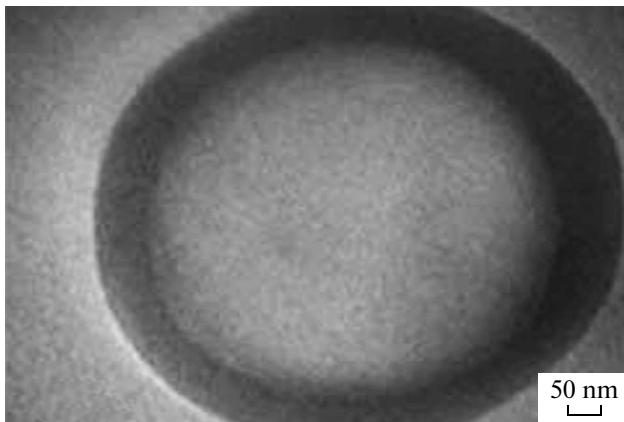


**Fig. 4.** TEM micrograph of the capsule produced in Exp. M1.

showed that the products had a size range of about 300–1300 nm and contained both magnetic capsules with core–shell morphology and PS solid particles as it is shown in Fig. 2. All particles are spherical in shape. The magnetite particles are visible as dark spots inside the spherical polystyrene capsules.

The TEM micrographs show that the encapsulation of the magnetic iron oxide in the polymeric capsules is complete; neither free magnetite nanoparticles nor magnetic-free polystyrene capsules were observed in Exp. M4 while TEM micrographs of Exp. M1–M3 showed that there were some polymeric capsules which did not have any magnetite (Figs. 3, 4). It may be related to incomplete dispersion of the magnetite within the styrene monomers.

To measure the size of the particles, a number of about 100 latex particles (from the TEM micrographs) were counted to calculate the  $d_n$  as number average ( $\sum n_i d_i / \sum n_i$ ) where  $d_i$  is diameter of latex particles and  $n_i$  is the number of polymer particle with  $d_i$  in diameter [29]. For M4 and M2 latexes, the  $d_n$  are 612 nm and 484 nm, respectively.

The distribution of the magnetite within the polystyrene capsules was quite heterogeneous. Although the magnetite particles were distributed apparently uniformly in the starting styrene system, they segregated and accumulated at one side of capsules during the miniemulsion preparation or the subsequent polymerization.

The magnetic emulsion is visibly brown and homogeneous. When the external magnetic field was applied to M2 latex, the magnetic latex was separated from the bulk emulsion. We also investigated the morphology of the latex particles of the prepared layer of the emulsion after magnetic separation for M2 latex, as shown in Fig. 5(A, B). In the layer of the emulsion after magnetic separation, there were only latex particles with  $\text{Fe}_3\text{O}_4$  nanoparticles.

To study the effect of initiator concentration on morphology of the latex, the experiments R1 and R2 were carried out. Polymerization of these miniemulsions led to two phase solution: hexadecane and magnetite at the oily phase in the top layer and the latex at the aqueous phase in the bottom layer. The primary suggestion of the fact would be that there was no significant encapsulation of hexadecane and  $\text{Fe}_3\text{O}_4$  within the capsules. The result was confirmed with TEM micrographs of the R1 and R2 latex. As shown in

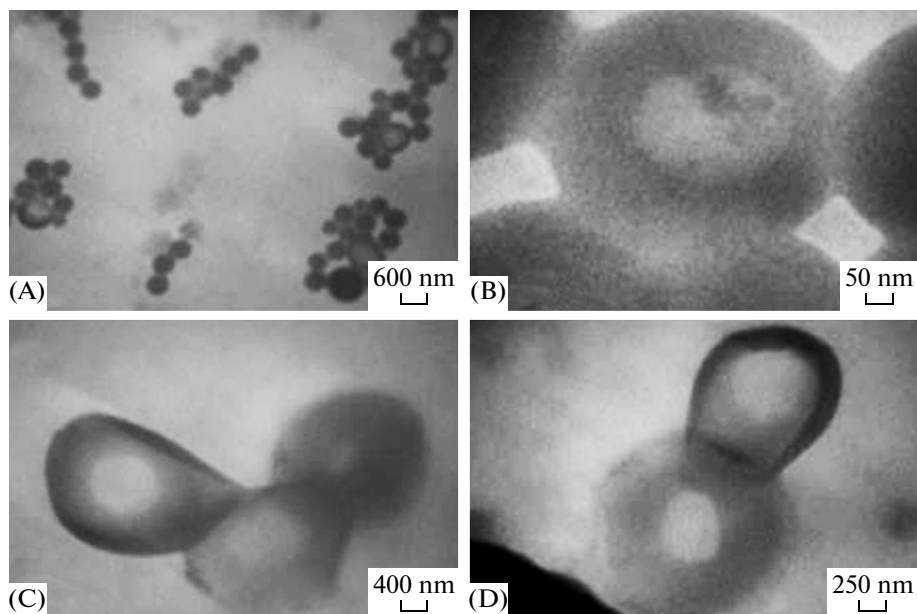


**Fig. 5.** TEM micrographs of the latexes produced in Exp. M2 after magnetic separation (A, B) and of the latexes produced in R-experiments (C, D).

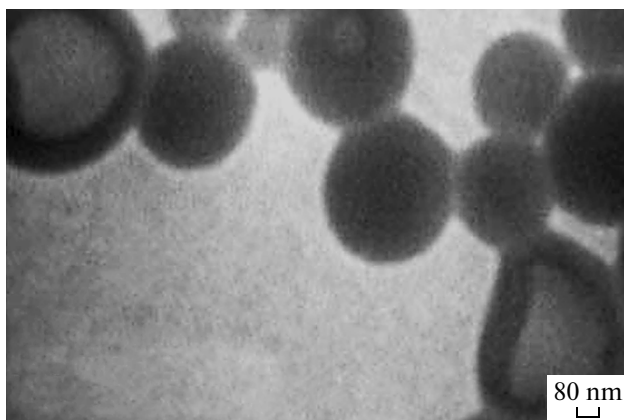


**Fig. 6.** TEM micrographs of the latexes produced in Exp. V.

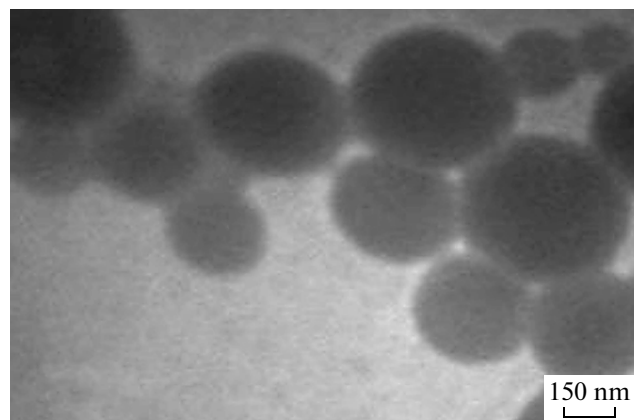


**Fig. 7.** TEM micrographs of the latexes produced in Exp. K.

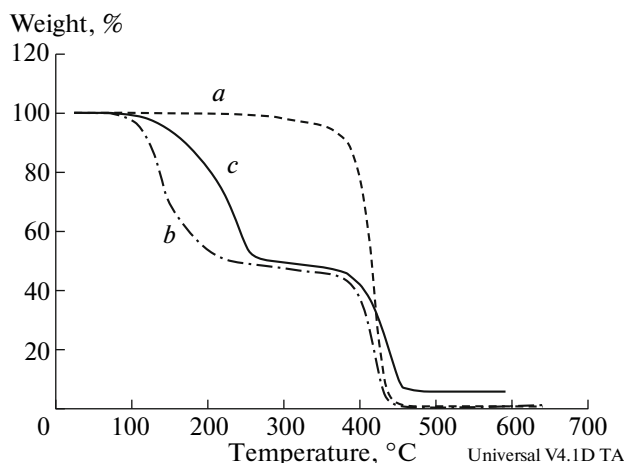


**Fig. 8.** TGA thermographs of the latexes produced in K, V and M4 experiments, curves *a*, *b*, and *c*, respectively.

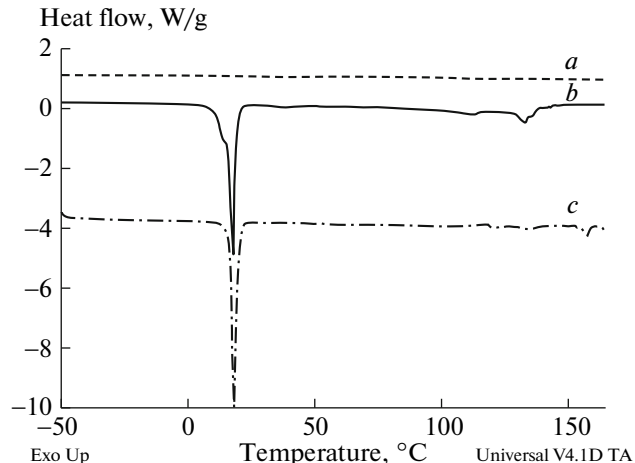


**Fig. 9.** DSC thermographs of the latexes produced in K, V and M4 experiments, curves *a*, *b*, and *c*, respectively.

Fig. 5(C, D) there was no complete encapsulation; some of the capsules were defective. This fact may be related to insufficient amount of initiator for producing the magnetic capsules.

The best encapsulation of magnetite and hexadecane within the PS capsules were obtained in Exp. M4 where the amount of magnetite in the monomer was 0.5 g (8.3% of monomer) and the amount of initiator was 0.2 g (3.3% of monomer). In M4 latex there were magnetic PS capsules with high magnetite loading and solid PS particles.

By decreasing the amount of magnetite from 0.5 g to 0.05 g the loading of magnetite within the capsules decreases.

For comparison, TEM micrographs of the V and K latexes are shown in Fig. 6 and Fig. 7, respectively.

Thermal properties of the produced latexes were investigated using DSC and TGA analyses (Table 2). The magnetite content of the magnetic latex could be estimated by thermogravimetric analysis under an ar-

gon atmosphere to minimize the mass increase due to iron oxidation. Herein, the polymer was completely decomposed at temperatures above 500°C and the magnetite content of the magnetic capsules was measured to be 5.6 wt % for M4 capsules (curve *c* in Fig. 8). Curves *b* and *a* are TGA thermographs of V and K latexes, respectively, and show less than 0.7% residue at 600°C.

In TGA thermographs of the M4 and V latexes there are two weight losses: the first in the range of 100–250°C, which is related to hexadecane evaporation and shows the proportion of hexadecane in the capsule (50.76% for M4 magnetic capsules and 52.71% for V capsules) and the second weight loss at about 300–450°C, which is related to PS destruction. In curve *a*, there is only one weight loss for PS decomposition.

DSC thermographs of the experiments M4, V, and K latexes (curves *a*, *b*, and *c*, respectively) are also given in Fig. 9. Curves *b* and *c* show that the products

**Table 2.** Heat of fusion for hexadecane, proportion of hexadecane, and residue amount of M4, V, and K latexes

Experiment	Heat of fusion for hexadecane in DSC, J/g	Proportion of hexadecane in the capsules from TGA, %	Residue amounts in TGA, %
M4	94.4	50.76	5.62
V	102.2	52.71	0.34
K	—	—	0.65

have two phase changes: the first for hexadecane melting over a temperature range of 6–22°C and a latent heat of fusion 102.2 J/g for V latex and 94.4 J/g for M4 latex (note that the melting point of hexadecane is about 18°C) and the second small peak at about 100°C, related to the glass transition of polystyrene. As can be concluded from the heat of fusion in DSC analyses and the residue up to 300°C in TGA, the amounts of hexadecane within the M4 capsules are less than those within the V capsules due to the presence of magnetite nanoparticles within M4 capsules.

## CONCLUSIONS

Stable magnetic nanocapsules with high magnetite loading were prepared via emulsifier-free miniemulsion polymerization. The best encapsulation of magnetite and hexadecane within the PS capsules were obtained where the amounts of magnetite and initiator in monomer were 8.3% and 3.3% of the monomer, respectively. The existence of magnetite and hexadecane in the capsules was proven by TEM, TGA, and DSC analyses. The capsules had a size range of about 300–1300 nanometers in diameter and the magnetite loading was reduced by decreasing the amount of magnetite in the starting monomer system.

## ACKNOWLEDGMENT

Special gratitude goes to Mr. Hashemi for obtaining TEM micrographs in the laboratory of electronic microscopy of University College of Science in the University of Tehran.

## REFERENCES

1. S. S. Davis and L. Illum, *Biomaterials* **9**, 111 (1988).
2. M. S. Romero-Cano and B. Vincent, *J. Control Release* **82**, 127 (2002).
3. M. Q. Slagt, S. E. Stiriba, R. G. M. Klein Gebbink, H. Kautz, H. Frey, and G. V. Koten, *Macromolecules* **35**, 5734 (2002).
4. D. Moinard-Checot, Y. Chevalier, S. Briancon, H. Fessi, and S. Guinebretiere, *J. Nanosci. Nanotech.* **6**, 2664 (2006).
5. J. Su, L. Wang, and L. Ren, *J. Appl. Polym. Sci.* **101**, 1522 (2006).
6. Y. Taguchi, H. Yokoyama, H. Kado, and M. Tanaka, *Colloid. Surf. A Physicochem. Eng. Asp.* **301**, 41 (2007).
7. C. Berkland, E. Pollauf, N. Varde, D.W. Pack, and K. Kim, *Pharm. Res.* **24**, 1007 (2007).
8. K. Krauel, L. Girvan, S. Hook, and T. Rades, *Micron* **38**, 796 (2007).
9. S. Lelu, C. Novat, C. Graillat, A. Guyot, E. Bourgeat-Lami, *Polymer International* **52**, 542 (2003).
10. M. M. Maye, Y. Lou, and C. J. Zhong, *Langmuir* **16**, 7520 (2000).
11. M. R. Grancio and D. J. Williams, *J. Polym. Sci. Part A-1* **8**, 2617 (1970).
12. Y. Frere, L. Danicher, and P. Gramain, *Eur. Polym. J.* **34(2)**, 193 (1998).
13. B. K. Kim, S. J. Hwang, J. B. Park, and H. J. Park, *J. Microencapsul.* **19(6)**, 811 (2002).
14. K. Landfester, *Annual Reviews of Material Research* **36**, 231 (2006).
15. F. Tiarks, K. Landfester, and M. Antonietti, *Macromol. Chem. Phys.* **202**, 51 (2001).
16. B. Erdem, E. D. Sudol, V. L. Dimonie, and M. El-Aasser, *J. Polym. Sci. Polym. Chem.* **38**, 4419 (2000).
17. K. Sugibayashi, Y. Morimoto, T. Nadai, and Y. Kato, *Chem. Pharm. Bull.* **25**, 3433 (1977).
18. E. Ciroonchatapan, M. Ueno, H. Sato, I. Adachi, H. Nagae, K. Tazawa, and I. Horikoshi, *Pharm. Res.* **12**, 1176 (1995).
19. P. K. Gupta and C. T. Hung, *Life Sci.* **44**, 175 (1989).
20. D. K. Kim, Y. Zhang, W. Voit, K. V. Rao, J. Kehr, B. Bjelke, and M. Muhammed, *Scr. Mater.* **44**, 1713 (2001).
21. M. Uhlen, *Nature* **340**, 733 (1989).
22. V. Holzapfel, M. Lorenz, C. K. Weiss, H. Schrezenmeier, K. Landfester, and V. Mailänder, *J. Phys. Condens. Matter* **18**, S2581 (2006).
23. I. Hilger, W. Andra, R. Hergt, R. Hiergeist, H. Schubert, and W. A. Kaiser, *Radiology* **218**, 570 (2001).
24. K. Landfester and L. P. Ramirez, *J. Phys. Condens. Matter* **15**, 1345 (2003).
25. L. P. Ramirez and K. Landfester, *Macromol. Chem. Phys.* **22**, 204 (2003).
26. V. Holzapfel, A. Musyanovych, K. Landfester, M.R. Lorenz, and V. Mailander, *Macromol. Chem. Phys.* **206**, 2440 (2005).
27. L. Torini, J. F. Argillier, and N. Zyドowicz, *Macromolecules* **38**, 3225 (2005).
28. R. Faridi-Majidi, N. Sharifi-Sanjani, and F. Agend, *Thin Solid Films* **515**, 368 (2006).
29. P. A. Lovell and M. S. El-Aasser, *Emulsion Polymerization and Emulsion Polymers* (Wiley, New York, 1999, Chapter 12).